Contents lists available at ScienceDirect

Heliyon

journal homepage: www.cell.com/heliyon

Research article

Epoxidised sesame oil as a biobased coupling agent and plasticiser in polylactic acid/thermoplastic yam starch blends

Rodrigo Ortega-Toro [a,*], Alex López-Córdoba [b], Felipe Avalos-Belmontes [c]

[a] Department of Food Engineering, Faculty of Engineering, Food Packaging and Shelf Life Research Group (FP&SL) and Complex Fluids Engineering and Food Rheology (IFCRA) Research Group, Universidad de Cartagena, Carrera 6 # 36-100, Cartagena de Indias D.T y C, Colombia
[b] Duitama Sectional Faculty, School of Agricultural Business Administrations. Universidad Pedagógica y Tecnológica de Colombia. Carrera 18 con Calle 22, Duitama 150461, Colombia
[c] Faculty of Chemical Sciences, Universidad Autónoma de Coahuila. V. Carranza s/n, 25000, Saltillo, Coahuila, Mexico

ARTICLE INFO

ABSTRACT

This work aims to improve the physicochemical properties of polylactic acid (PLA) and thermoplastic yam starch (TPS) blends using epoxidised sesame oil (ESO). We used epoxidised sesame oil from two Colombian Caribbean crops: *Dioscorea rotundata* and *Sesamum indicum*, with an oil substitution of 58.4 %. Films were obtained through extrusion and compression moulding processes. Moisture content, solubility, contact angle, and mechanical, barrier, and structural properties were determined using optical and scanning electron microscopy, infrared Fourier transform spectroscopy. Thermal analyses were also performed using thermogravimetry and differential scanning calorimetry techniques. The results suggest that the PLA and TPS interactions can be improved with the addition of ESO as coupling agent, enhancing the interfacial adhesion between the polymers, and favouring the smoothness of the film surface. Furthermore, the ESO addition led to increased thermal stability while restricting molecular mobility, indicating a coupling agent effect. In conclusion, the use of epoxidised oil for preparing films based on high PLA content and TPS allows obtaining enhanced interfacial adhesion. Considering the above, the developed materials have potential application in semi-rigid food packaging.

1. Introduction

Petroleum-based plastics are globally used in a wide range of applications (e.g., packaging, construction, textiles, medical devices, transport, among others) due to their durable and versatile advantages. However, improper management of plastic waste has resulted in adverse environmental impacts (Rodrigues et al., 2005). Bio-based and biodegradable plastics such as polylactic acid (PLA) and thermoplastic starch have gained special attention in the last years because their abundance, renewability, non-toxicity and relatively low cost. Besides, these polymers can be degraded by common microorganisms into natural substances such as water, carbon dioxide, and organic matter.

PLA is a synthetic and aliphatic polyester made from lactic acid, which is a natural monomer derived from starch- or sugar-containing agricultural products. Because of its commercial availability, excellent processability, high transparency, and water solubility resistance, PLA results of great interest in materials manufacturing (Pankaj et al., 2014). Nevertheless, it is brittleness and shows low degradation rate as well as low thermal resistance, which limits its application (Pankaj et al., 2014). To overcome its low degradation rate, PLA is blended with other natural polymers having higher degradation rates such as starches (Akrami et al., 2016). Particularly, starches isolated from yam (*Dioscorea rotundata*) are considered attractive because of their nutritional value and film-forming properties (Da Costa et al., 2020).

On the other hand, while starch is hydrophilic, PLA is hydrophobic, making the use of compatibilisers necessary to increase the interfacial adhesion between them (Vachon et al., 2017). In the past, several compatibilisers for PLA/starch blends were studied, including grafted copolymers such as poly (ε-caprolactone), maleic anhydride and polyethene glycol (Akrami et al., 2016; Collazo-Bigliardi et al., 2019). Since epoxidised vegetable oils are non-toxic and abundant, they were proposed as bio-based compatibiliser and plasticisers in PLA-containing blends (Zhang et al., 2017). Balart et al. (2016) studied the effect of adding epoxidised linseed oil (ELO) on the properties of PLA/hazelnut shell flour composites. The latter authors find that ELO could act as a compatibiliser, improving the matrix-filler interactions and reducing the

---

* Corresponding author.
E-mail address: rortegap1@unicartagena.edu.co (R. Ortega-Toro).

fragility of the composites. Similarly, Carbonell-Verdu et al. (2017) observed a plasticisation effect of epoxidised cottonseed oil (ECSO) on poly (lactic acid). Meanwhile, García-García et al. (2020) reported that epoxidised Karanja oil may improve the ductility and the thermal stability of PLA films.

Sesame oil is rich in unsaturated fatty acids and natural antioxidants. Nevertheless, both sesame seeds and oil can cause allergic responses in certain people. Moreover, sesame oil use is limited due to its low-temperature decomposition. Because of the high content of oleic and linoleic acids, sesame oil is suitable for *in situ* epoxidation using peracetic acid.

In this work, we assayed epoxidised sesame oil (ESO) as a plasticiser and compatibiliser in PLA/thermoplastic yam starch (TPS) films obtained by extrusion and compression moulding. PLA/TPS composites with and without ESO were prepared and characterised in terms of its morphology, thickness, moisture content, water vapour permeability, surface hydrophobicity, water-solubility, chemical conformation, tensile properties, and thermal properties. PLA and TPS films were also analysed for comparison purposes.

2. Materials and methods

2.1. Materials

Yam (28.3% amylose and 71.7 % amylopectin content) and sesame seeds were purchased from the local market in Cartagena de Indias (Colombia); PLA (LL700, 1.25 g cm^{-3} density) was supplied by Natureworks (U.S.A). Glycerol used as a thermoplastic starch plasticiser, and other reagents were provided by Sigma-Aldrich and Panreac (Bogotá-Colombia).

2.2. Obtention of blends based on PLA and TPS polymers

The ESO was obtained by adding polar groups to the chemical sesame oil structure, which was achieved through homogeneous catalysis with peroxyacetic acid, as described in previous works (Gómez-Contreras et al., 2020). Briefly, the catalyst solution was added into the reactor, previously dissolving the acetic acid (A.A.) in the oxidant (hydrogen peroxide: H.P.). In this way, 34 g of virgin sesame oil was charged with 33 g of H.P. (50 wt %), 31 g of A.A. (16 wt %) and 1 g of sulfuric acid (97 wt %). The operating conditions were 60 °C, 300 rpm and 1 atm for 180 min. The amounts and reaction conditions were adjusted according to preliminary experiments. The main objective of the oil epoxidation is that the obtained polar part can interact with the thermoplastic starch, and the nonpolar part could interact with PLA.

To prepare the PLA/TPS-based blends, Yam starch and glycerol were mixed at a ratio of 1:0.25 (w/w) to plasticise the starch and obtain the thermoplastic version. Then, TPS was obtained through an extrusion process, in the temperature range 80–130 °C from the feed section to the outlet section of the equipment. Then, a second extrusion was performed blending TPS and PLA with or without ESO with a degree of substitution of 58.4 %. Blends were adjusted according to the formulations shown in Table 1, pelletised and conditioned at 53% relative humidity (R.H.) and 25 °C until pressing. Finally, the obtained pellets were preheated and then, pressed at 130 °C for 10 min according to Ortega-Toro et al. (2014,

2015b and 2016a, b). The resulting films were cooled and conditioned at 53 % R.H. and 25 °C until characterisation.

A simple classification factorial design with five formulations in total was performed. As controls, PLA and TPS polymers were used. The formulations were chosen to have two pure controls: TPS and PLA. A mixture of such polymers was prepared in the absence of ESO, as well as two other blends with either 1.5 % or 3 % ESO. The effect of ESO was observed, and the properties of the pure materials were compared.

2.3. Characterizations of the obtained films

2.3.1. Moisture content

Films samples were conditioned at 53 % R.H. and the humidity content was monitored for 24 h using a convection stove at 70 °C Eq. (1) (Gurler et al., 2020) was used to calculate the relationship between wet and dry weight. The assays were performed in triplicate.

$$\% \ M.C. = \frac{Pa}{Pt} \times 100 \tag{1}$$

where: *% M.C.* is the moisture content expressed as a percentage; *Pa* is the existing water weight (initial weight - final weight), and *Pt* is the total weight of the dry sample.

2.3.2. Water solubility

The water solubility (WS) of the films was determined by their immersion for 48 h in distilled water, using a water ratio of 1:10 (w/w). Then, the film samples were taken to a natural convection stove for 24 h at 70 °C to remove the water. The solubility of the films was calculated from the initial weights (Wi) and final weights (Wf) using Eq. (2) (Ballesteros-Martínez et al., 2020). This test was performed in triplicate.

$$\%WS = [(Wi - Wf)Wi] \times 100 \tag{2}$$

2.3.3. Contact angle with water

The contact angle was calculated analysing the shape of a distilled water drop (0.01 mL) after 10 s of contact with the film surface. A white background digital camera was used to take a photo of the water drop —a 50-cm distance was considering between the camera lens and the drop —. Subsequently, image analysis was performed using the Goniotrans Pro-APK software (Ortega-Toro et al., 2015a).

2.3.4. Tensile properties

Prior to the determination of the mechanical properties, samples were cut and subjected to 25 °C (53 % R.H.) for 48 h (Tensile Strength, Elastic Modulus and Elongation at a breakpoint). Mechanical tests were based on ASTM D882 (Sothornvit et al., 2007). The stress at break, percentage of elongation and Young's modulus were determined at a spindle speed of 10 mm min^{-1} using a universal testing machine equipped with a 500N cell. Besides, the thickness was measured with a micrometre taking seven random measurements per film.

2.3.5. Water vapour permeability (WVP)

According to previous studies (Park et al., 2000; Ortega-Toro et al., 2014) and based on the ASTM E96-95 standard method, water vapour permeability was calculated using a humidity gradient of 53–100 % H.R. at 25 °C.

Table 1. Mass fraction of studied formulations.

Formulations	PLA	TPS	Glycerol	Epoxidized sesame oil
PLA	1.000	0.000	0.000	0.000
TPS	0.000	0.800	0.200	0.000
PLA$_{75}$/TPS$_{25}$	0.706	0.235	0.059	0.000
PLA$_{75}$/TPS$_{25}$/ESO$_{1.5}$	0.696	0.232	0.058	0.014
PLA$_{75}$/TPS$_{25}$/ESO$_3$	0.686	0.229	0.057	0.027

Table 2. Mean values and standard deviation of thickness (μm), moisture content (g of water/100g dry film), solubility in water (g soluble film/100g dry film), contact angle (°) and water vapor permeability (g· mm/kPa·h·m^2) of the studied formulations conditioned at 53% R.H. and 25 °C.

Formulations	Thickness	Moisture	Solubility in water	Contact angle	Water vapor permeability
PLA	175 ± 26^a	0.36 ± 0.05^a	0.30 ± 0.09^a	63.3 ± 1.5^d	0.36 ± 0.11^a
TPS	439 ± 34^c	11.0 ± 0.8^d	28.4 ± 0.8^c	52.3 ± 0.6^a	9.43 ± 0.76^d
PLA$_{75}$/TPS$_{25}$	198 ± 34^b	3.7 ± 0.5^c	6.6 ± 0.9^b	61.7 ± 2.5^c	2.30 ± 0.87^c
PLA$_{75}$/TPS$_{25}$/ESO$_{1.5}$	181 ± 17^{ab}	3.1 ± 0.4^{bc}	6.3 ± 1.7^b	61.0 ± 2.6^c	1.52 ± 0.33^b
PLA$_{75}$/TPS$_{25}$/ESO$_3$	176 ± 21^a	2.7 ± 0.6^b	6.7 ± 0.3^b	55.5 ± 0.7^b	1.36 ± 0.26^b

Different superscript letters mean significant differences ($p < 0.05$) between formulations.

2.3.6. Structural properties (HRMO, SEM and FTIR)

The structural properties were studied on the surface of films using a High-Resolution Optical Microscopy (HRMO). The obtained microphotographs were analysed and processed using the Image Pro-Plus Software version 5.1.

Additionally, cross-section and surface micrographs of the films were obtained by Scanning Electron Microscopy (SEM), using a JEOL JSM-5410 microscope (Japan). The film samples were kept in desiccators with P$_2$O$_5$ for two weeks to remove the strongly bound water. Subsequently, the films were frozen using liquid nitrogen and cryo-fractured to observe the cross-section. The films were then fixed on copper slides, gold-coated, and observed using an accelerating voltage of 10 kV.

FTIR spectra of the films were obtained to determine chemical modifications resulting from the ESO incorporation into the polymer blend. The spectra were performed between 4000 and 800 cm^{-1} at a resolution of 4 cm^{-1}.

2.3.7. Thermal analysis (TGA and DSC)

Samples of 5.5 mg approximately per formulation were studied by thermogravimetry (TGA). Thermogravimetric analysis was performed in a temperature range of 30–800 °C using a HiRes TGA 2950 TA Instruments TGA at 20 $°C\ min^{-1}$.

On the other hand, Differential Scanning Calorimetry (DSC) analysis was carried out on samples of about 8 mg using a TA Instruments DS100 QC Kit.

Curves were processed using OriginPro 8.0 Software and Geogebra 3D.

2.3.8. Statistical analysis

The collected data was analysed using Statgraphics Plus Software (Manugistics Corp., Rockville, MD. U.S.A.). An analysis of variance (ANOVA) was performed and Fisher's least significant difference (LSD) tests at the 0.05 level of significance was used.

3. Results and discussion

3.1. Thickness and moisture content

TPS films showed a thickness 2.8-fold higher than that of the PLA ones ($p < 0.05$) (Table 2). The latter could be attributed to the higher fluence in the thermo-compression process of PLA, regarding TPS films. In comparison with PLA films, PLA$_{75}$/TPS$_{25}$ films showed an increase in thickness, whereas PLA$_{75}$/TPS$_{25}$/ESO$_3$ samples showed a similar thickness (Table 2), suggesting better compatibility of the last system. According to Ferri et al. (2016), epoxidation increases the polarity and stability of vegetable oils, improving their compatibility with polymers and enhancing their energetic interaction with the matrix. Regarding the PLA$_{75}$/TPS$_{25}$/ESO$_{1.5}$ films, the compatibility of the system was not significantly improved probably due to a low ESO concentration (Table 2).

As expected, PLA films showed the lowest moisture content, which could be explained by their hydrophobic character. In contrast, films based on TPS (i.e., a hydrophilic biopolymer) showed the highest moisture content (Table 2). PLA$_{75}$/TPS$_{25}$ films showed higher moisture content than the PLA ones because of the presence of TPS. However, the addition of 3 % ESO led to a moisture content decrease of around 27% in films ($p < 0.05$) (Table 2). This behaviour may be because the ESO addition improved the intermolecular cohesivity of the polymeric matrix, decreasing the availability of water-binding sites and delaying the diffusion of water molecules through the composite material (Moo-Tun et al., 2020).

3.2. Water solubility, contact angle, and water vapour permeability

TPS films showed values of water solubility around 28.4 % (Table 2). Comparable results were previously reported for corn starch (25.4 %) and gelatine (26.13 %) films (Pimentel et al., 2018).

In agreement with Sharif et al. (2019), PLA films showed low values of water solubility (0.3 %). The water solubility of composite films was around 6.5 %. No significant differences were found between the films with and without ESO ($p > 0.05$) (Table 2). The increase in water solubility of the composite films in comparison with the PLA ones was attributed to the presence of starch.

The contact angle provides the surface hydrophobicity of films. It is well known that the higher contact angle value, the higher surface hydrophobicity. As expected, TPS films showed lower values of contact angle than PLA films (Table 2). This behaviour may be because TPS films have a higher amount of hydrophilic group (e.g., O–H groups of glycerol and starch) and then higher water affinity (Belhassen et al., 2014), as compared with PLA films. The PLA$_{75}$/TPS$_{25}$, PLA$_{75}$/TPS$_{25}$/ESO$_{1.5}$, and PLA$_{75}$/TPS$_{25}$/ESO$_3$ films showed a more hydrophilic surface (i.e., lower values of contact angle) than the PLA ones (Table 2). Besides, PLA$_{75}$/TPS$_{25}$/ESO$_3$ films showed lower values of contact angle than the other composite materials (Table 2). These results suggest that polar epoxide

Table 3. Mean values and standard deviation of the elastic modulus (EM), tensile strength (TS) and deformation of the studied films (E) conditioned at 53% R.H. and 25 °C.

Formulations	EM (MPa)	TS (MPa)	E (%)
PLA	1276 ± 84^c	48 ± 3^e	4.5 ± 0.3^b
TPS	95 ± 12^a	8.1 ± 1.1^a	35 ± 5^c
PLA$_{75}$/TPS$_{25}$	1123 ± 12^b	29.1 ± 0.8^d	3.8 ± 0.2^a
PLA$_{75}$/TPS$_{25}$/ESO$_{1.5}$	1105 ± 11^b	25.4 ± 0.5^c	4.8 ± 0.5^b
PLA$_{75}$/TPS$_{25}$/ESO$_3$	1094 ± 9^b	23.1 ± 0.7^b	5.3 ± 0.3^b

Different superscript letters mean significant differences ($p < 0.05$) between formulations.

PLA

TPS

PLA$_{75}$/TPS$_{25}$

PLA$_{75}$/TPS$_{25}$/ESO$_{1.5}$
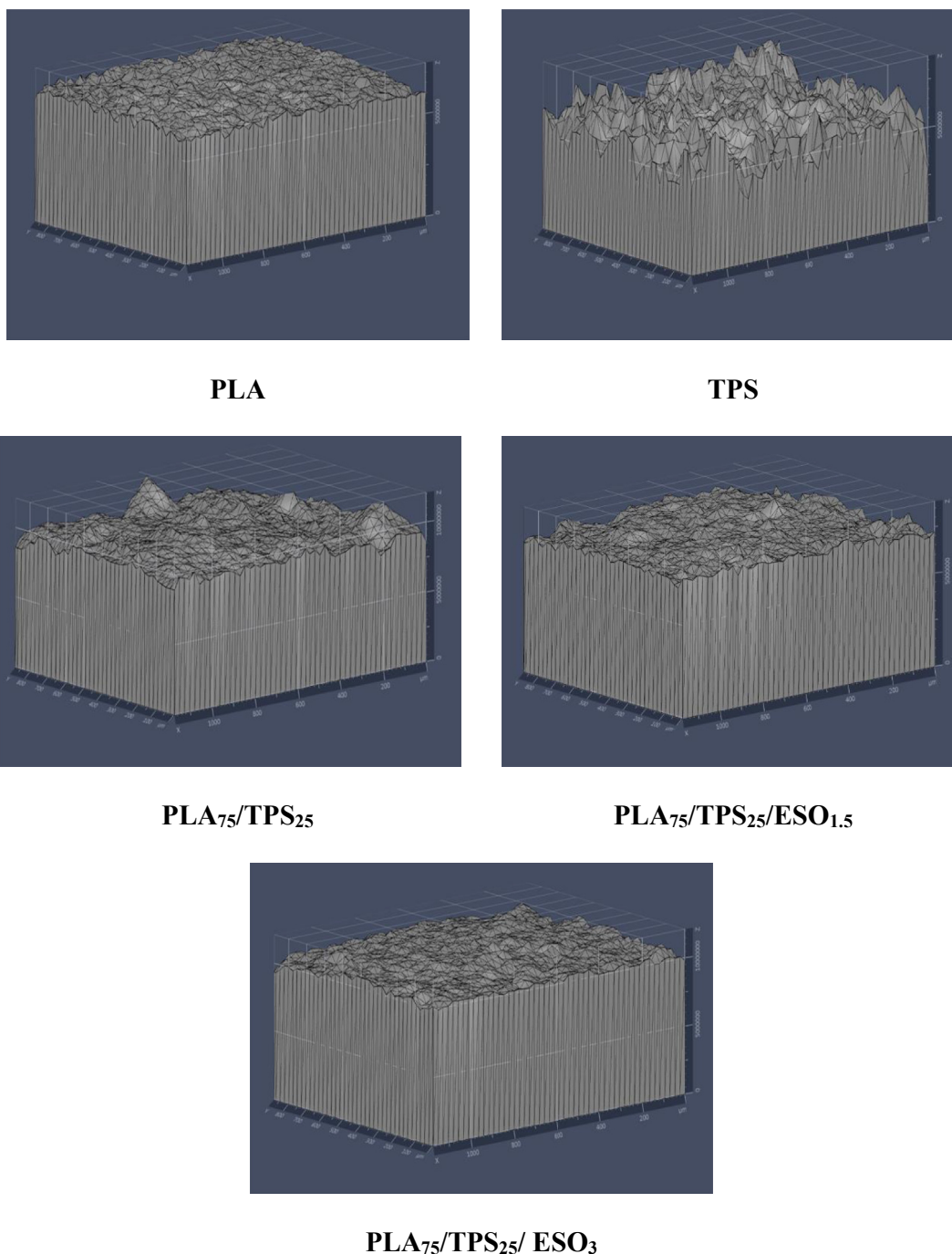
PLA$_{75}$/TPS$_{25}$/ ESO$_3$

Figure 1. Surface optical micrographs of the studied films (40X) conditioned at 53% R.H. and 25 °C.

groups of ESO were mainly oriented towards the film surface, increasing their hydrophilic character.
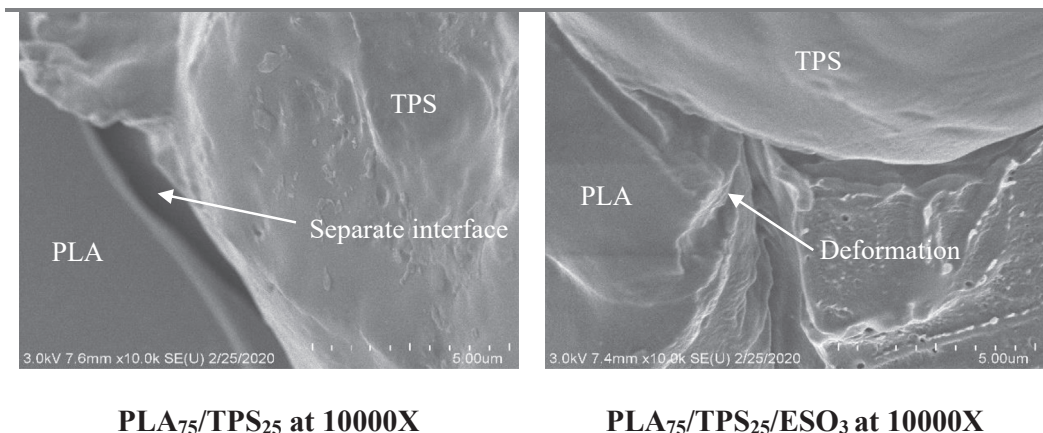
TPS and PLA films showed WVP values of 9.43 g mm $(kPa \cdot h \cdot m^2)^{-1}$ and 0.36 g mm $(kPa \cdot h \cdot m^2)^{-1}$, respectively (Table 2). Similar results were for cassava starch (13.2 g mm $(kPa \cdot h \cdot m^2)^{-1}$) (Valencia-Sullca et al., 2018) and PLA (0.44 g mm $(kPa \cdot h \cdot m^2)^{-1}$) films (Tampau et al., 2020). PLA$_{75}$/TPS$_{25}$ films showed higher WVP values than the PLA ones. However, the ESO addition decreased WVP of films by approximately 37 %. These results agree with the hydrophilicity behaviour of the surface, the water content and the thickness of the films above discussed suggesting that ESO acts as a coupling agent in PLA/TPS blends (Frone et al., 2016; Akrami et al., 2016; Muller et al., 2016). According to Balart et al. (2016), epoxidised oil acts as a coupling agent through chemical

reactions among its epoxy groups, PLA hydroxyl groups and other molecules such as cellulose or starch.

3.3. Tensile properties

The elastic modulus (EM), tensile strength (TS), and strain at break of the studied films (E) are shown in Table 3. TPS and PLA films showed elastic modulus values of 95 MPa and 1276 MPa, respectively. All composite films showed a similar decrease in the elastic modulus values in comparison with the neat PLA film, regardless of the presence of ESO. TPS and PLA films showed values of tensile strength and deformation, as reported previously (Mirkhalaf et al., 2019).

Cross-section micrographs

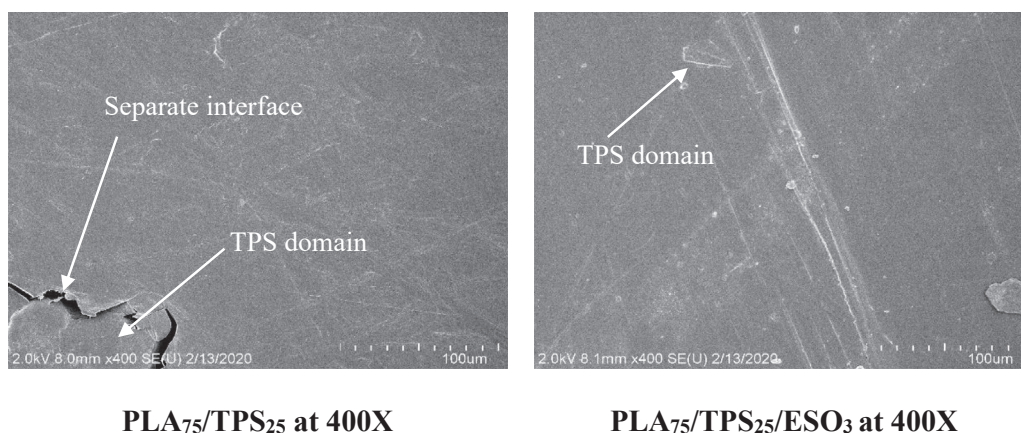**PLA$_{75}$/TPS$_{25}$ at 10000X**   **PLA$_{75}$/TPS$_{25}$/ESO$_3$ at 10000X**

Surface micrographs

PLA$_{75}$/TPS$_{25}$ at 400X   **PLA$_{75}$/TPS$_{25}$/ESO$_3$ at 400X**

Figure 2. Cross-section SEM micrographs of studied films without epoxidized oil (PLA$_{75}$/TPS$_{25}$) and with epoxidized oil (PLA$_{75}$/TPS$_{25}$/ESO$_3$).

The composite films containing ESO (PLA$_{75}$/TPS$_{25}$/ESO$_{1.5}$ and PLA$_{75}$/TPS$_{25}$/ESO$_3$) showed a decrease in the tensile strength and an increase in the strain at break, as compared with the PLA$_{75}$/TPS$_{25}$ film (p < 0.05). Therefore, it could be stated that ESO can act as a plasticiser causing greater flexibility. García-García et al. (2020) studied the properties of PLA films supplemented with different amounts of epoxidised Karanja oil (EKO). Such authors find that EKO was able to act a plasticiser, decreasing the stress at break and increasing the strain at break. Similar behaviours were reported by other authors (Ferri et al., 2016; Carbonell-Verdu et al., 2017).

3.4. Morphological analysis

Figure 1 shows the micrographs of the surface of the different films studied. PLA films showed a homogeneous and smooth surface; whereas the PLA$_{75}$/TPS$_{25}$ ones had rougher surface probably due to the incompatibility between PLA and TPS polymers. The ESO addition was a useful way to decrease surface heterogeneity in composite films. In this sense, PLA$_{75}$/TPS$_{25}$/ESO$_{1.5}$ and PLA$_{75}$/TPS$_{25}$/ESO$_3$ showed a lower surface roughness, similar to the neat PLA films (i.e., improved compatibility). Yang et al. (2014) reported comparable results using epoxidised soybean oil as a plasticizer for ethylcellulose film preparation.

Cross-section and surface micrographs of the films are shown in Figure 2. An interface separation occurred in PLA$_{75}$/TPS$_{25}$ films, which could be attributed to low compatibility between the matrix components. In contrast, when ESO was used, a homogeneous surface was observed in PLA$_{75}$/TPS$_{25}$/ESO$_3$ films, lacking phase separations. The surface micrographs of films without ESO revealed TPS domains more prominent than those of films with ESO. Moreover, the phase separation was marked in films without ESO, while it was smooth in films with ESO. Similar results were obtained by Turco et al. (2019) when worked with poly (lactic acid)/thermoplastic starch films containing cardoon seed epoxidised oil and by Balart et al. (2016) when worked with composites based on PLA and hazelnut shell flour (HSF) with epoxidised linseed oil. Our results are also in agreement with those observed by Carbonell-Verdu et al. (2017) in PLA films containing maleinised cottonseed oil.

3.5. Infrared spectra

TPS films showed characteristic bands of yam starch around 3330 cm^{-1} (O–H stretching), 2933 cm^{-1} (C–H stretching from alkyl groups), 1655 cm^{-1} (H$_2$O bending vibration), 1455 cm^{-1} (C–H bending), 1242 cm^{-1} (C–O stretching), 1204 cm^{-1} (C–OH stretching), 1149 cm^{-1} (C–O stretching of the —C—O—H), 1103 cm^{-1} (C–O–H stretching), 1086 cm^{-1} (C–O bond stretching of the —C—O—C), and 991 cm^{-1} (CH$_2$
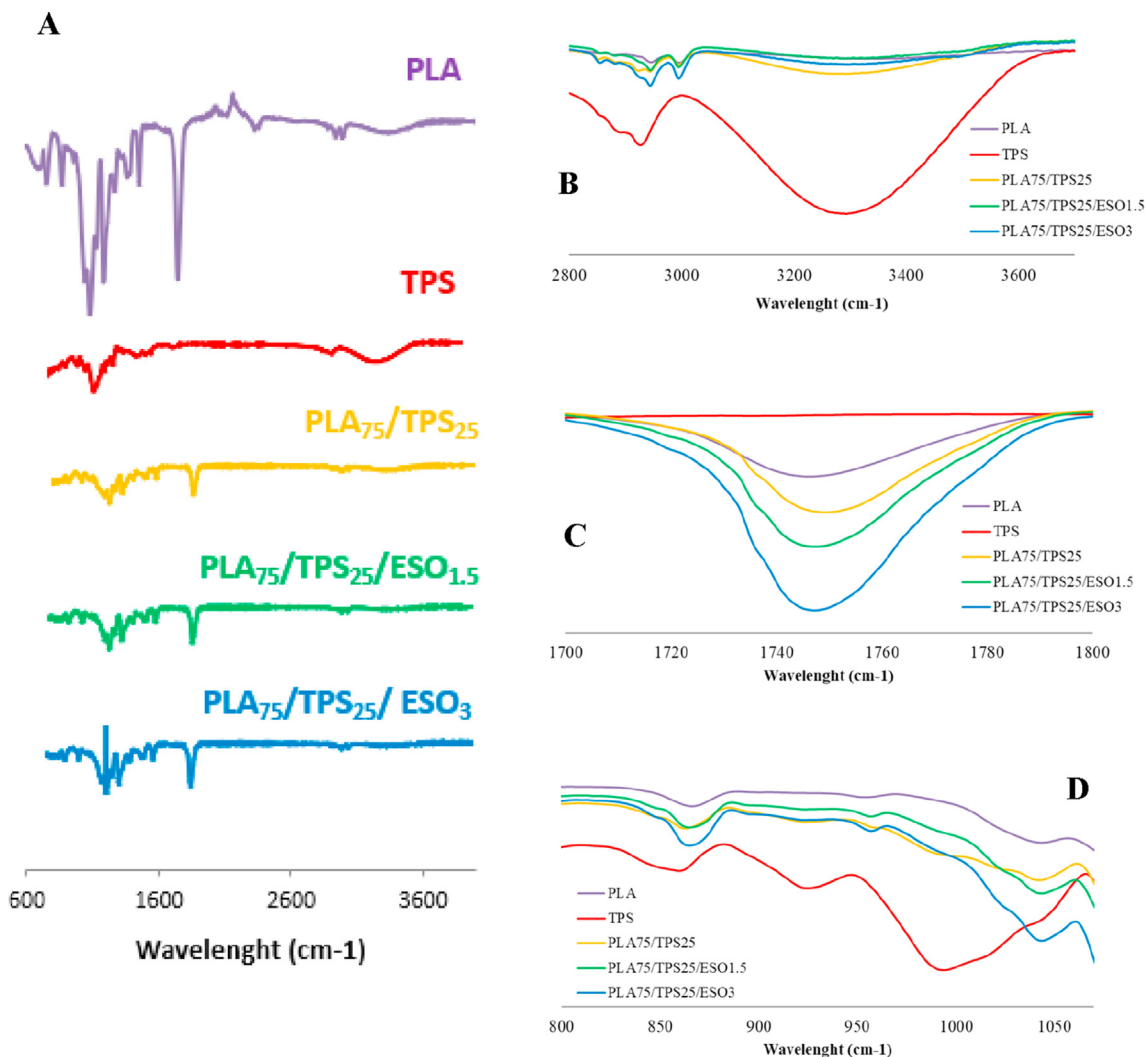
Figure 3. FTIR Spectra of studied films with and without epoxidized oil conditioned at 53% R.H. and 25 °C: A) Complete FTIR spectra; B) FTIR spectra section between 2800 cm^{-1} and 3700 cm^{-1}; C) FTIR spectra section between 1700 cm^{-1} and 1800 cm^{-1} and D) FTIR spectra section between 800 cm^{-1} and 1070 cm^{-1}

bending) (Figure 3). Andrade et al. (2017) reported similar results. PLA films showed the typical signal associated with the C–H asymmetric and symmetric stretching vibration around 2997 and 2947 cm^{-1} (Gurler et al., 2020). Moreover, IR spectra showed the typical stretching of the carbonyl group (—C=O) at 1750 cm^{-1} by lactide, and the —C—O— bond stretching in —CH—O— a group of PLA at 1182 cm^{-1} (Figure 3). PLA$_{75}$/TPS$_{25}$, PLA$_{75}$/TPS$_{25}$/ESO$_{1.5}$ and PLA$_{75}$/TPS$_{25}$/ESO$_{3}$ films showed characteristic signals of PLA and starch polymers, as well as some peaks overlapped. The signals corresponding to the epoxidized sesame oil were not detected because they were hampered by the vibrational peaks of the polymeric matrix.

3.6. Thermal properties of the films

Thermogravimetric curves and the maximum degradation temperatures of the studied films are shown in Figure 4 and Table 4, respectively. TPS films showed a thermal degradation pattern similar to that described in the literature for starch films supplemented with glycerol as a plasticiser. The mass loss observed between 70 and 180 °C was attributed to water evaporation, and the mass loss detected between 200 and 300 °C correspond to the glycerol-rich phase decomposition (Figure 4) (Khosravi et al., 2020; Gutiérrez et al., 2017; Herniou et al., 2019). The oxidation of the partially decomposed polymer chains took place at temperatures above 300 °C (Figure 4).

The thermal degradation of PLA films followed the typical pattern described in literature exhibiting the major weight loss between 280 and 375 °C (Figure 4), with a maximum degradation at 315.6 °C (Table 4) (Pankaj et al., 2014). In the PLA$_{75}$/TPS$_{25}$ and PLA$_{75}$/TPS$_{25}$/ESO$_{1.5}$ samples, the maximum degradation temperature was found to shift towards higher values (~342 °C), indicating higher thermal stability (Table 4). PLA$_{75}$/TPS$_{25}$/ESO$_{3}$ films showed lower degradation temperature (~329.7 °C), as compared with PLA$_{75}$/TPS$_{25}$ and PLA$_{75}$/TPS$_{25}$/ESO$_{1.5}$ ones (Table 4). The latter observation agrees with the fact that epoxidised sesame oil act as a plasticiser of the polymeric matrix, prompting the mobility of the polymer chains and decreasing the maximum degradation temperature (Balart et al., 2016; Sudha et al., 2017; Liu et al., 2018).

Table 4 shows the results obtained in the second DSC heating scan to avoid the effects of the thermal history of the composites. The glass transition temperature (Tg) was observed in all samples containing PLA., The Tg was 54.24 °C for pure PLA, and 50.6 °C for PLA/TPS blends. Similar trends were reported in previous studies for blends made of TPS and 20 % PLA (Collazo et al., 2019). The decreased Tg observed after the mixture of TPS and PLA polymers could be attributed to a plasticising effect exerted by TPS in the PLA matrix. Such effect may be achieved through the increase of the free volume in the matrix allowing the molecular mobility of the polymers (Mikus et al., 2014). When 3% ESO used in the PLA/TPS blend, it was observed a
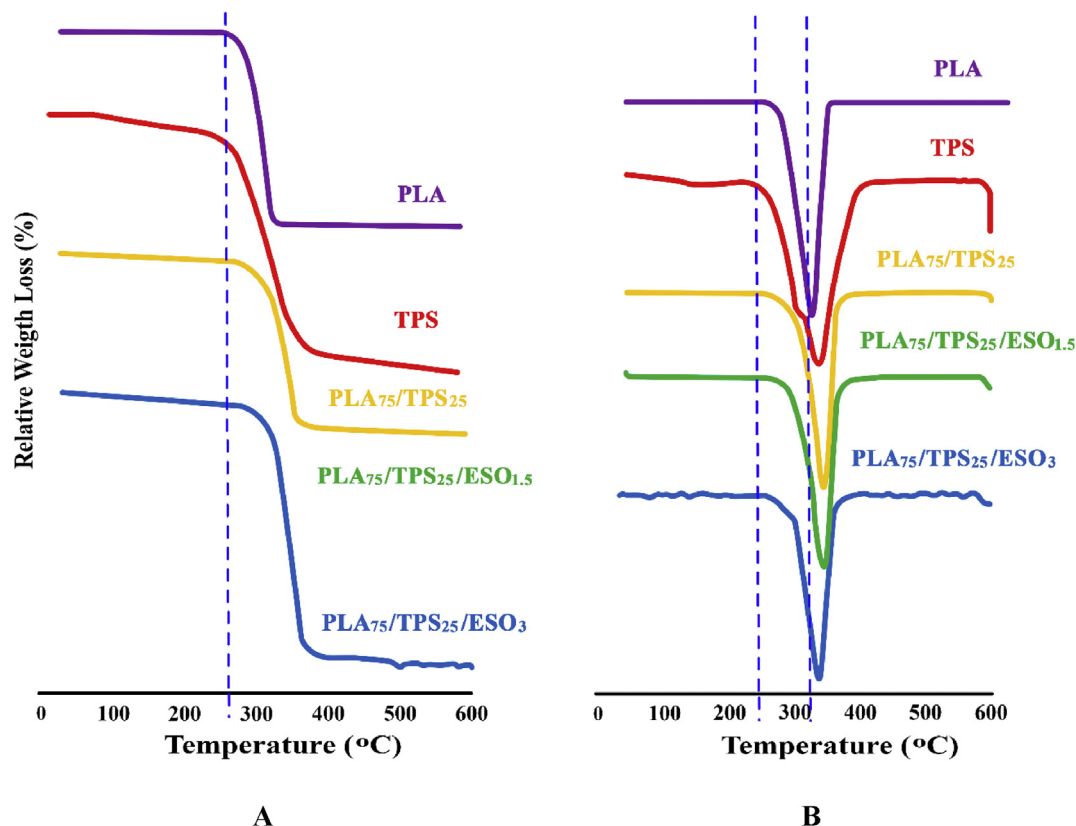
Figure 4. Thermogravimetry of the studied films conditioned at 53% R.H. and 25 °C: A) Thermogravimetric curve "TG"; B) Thermogravimetric curve first order derivative "DTG".

Table 4. Mean values and standard deviation of parameters obtained by DSC (glass transition temperature of PLA) and TGA (Maximum degradation temperature (T_{Peak}) and Initial degradation temperature (T_0)) of studied films conditioned at 53 % R.H. and 25 °C.

Formulations	DSC	TGA	
	Tg (°C)	T_{Peak} (°C)	T_0 (°C)
PLA	54.24 ± 0.3^b	315.6 ± 0.5^a	245.0 ± 0.2^b
TPS	—	337.5 ± 1.1^c	236.1 ± 0.5^a
PLA_{75}/TPS_{25}	50.6 ± 0.5^a	342.4 ± 0.9^d	267.33 ± 0.5^c
$PLA_{75}/TPS_{25}/ESO_{1.5}$	57.2 ± 1.6^c	341.3 ± 0.5^d	265.95 ± 0.3^c
$PLA_{75}/TPS_{25}/ESO_3$	57.9 ± 1.3^c	329.7 ± 0.5^b	285.13 ± 0.5^d

Different superscript letters mean significant differences (p < 0.05) between formulations.

significant increase in the Tg (up to 57.9 °C). The latter is a typical effect of coupling agents that restrict molecular mobility by increasing chemical interactions (Collazo et al., 2019). These results are accordance with that stated in previous sections where it was mentioned that the epoxy groups of ESO could interact with the hydroxyl groups of PLA and TPS polymers, restricting their mobility and promoting the increase of Tg.

4. Conclusions

Films made of polylactic acid with a low content of thermoplastic yam starch were obtained by extrusion and compression moulding. Epoxidised sesame oil was added to improve the interface and compatibility of the polymer blends. Addition of 3% ESO promoted a moisture content decrease and a surface wettability increase in materials, whereas the barrier against water vapour was increased. The PLA/TPS blends with and without ESO were rigid and tough, with little

deformability and values closer to pure PLA than to pure TPS. The addition of epoxidised oil increased deformation and loss of stiffness and tensile strength, indicating that it could act as a plasticiser for PLA.

According to results, the ESO addition may reduce the topographic accidents of the material, giving it higher smoothness. Moreover, the interfacial adhesion of the materials increased, observing a phase fading effect, which suggests that the epoxidised oil acts as an effective coupling agent. Furthermore, the addition of ESO to the material increased its thermal stability, while the epoxidised oil restricted the molecular mobility. The latter was related to the increase in Tg, indicating a coupling agent effect. As noted, the addition of epoxidised oil to bio-based matrices significantly improves properties, resulting in materials suitable for packaging low-moisture foods served at room temperature. This work shows a procedure to take advantage of the autochthonous resources to obtain biodegradable materials.

Declarations

Data availability statement

Data included in article/supplementary material/referenced in article.

Declaration of interests statement

The authors declare no conflict of interest.

Additional information

No additional information is available for this paper.

References

Akrami, M., Ghasemi, I., Azizi, H., Karrabi, M., Seyedabadi, M., 2016. A new approach in compatibilization of the poly (lactic acid)/thermoplastic starch (PLA/TPS) blends. Carbohydr. Polym. 144, 254–262.

Andrade, L.A., Alves Barbosa, N., Pereira, J., 2017. Extraction and properties of starches from the non-traditional vegetables yam and taro. Polimeros 27 (2), 151–157.

Balart, J.F., Fombuena, V., Fenollar, O., Boronat, T., Sánchez-Nacher, L., 2016. Processing and characterization of high environmental efficiency composites based on PLA and hazelnut shell flour (HSF) with biobased plasticizers derived from epoxidized linseed oil (ELO). Compos. B Eng. 86, 168–177.

Ballesteros-Mártinez, L., Pérez-Cervera, C., Andrade-Pizarro, R., 2020. Effect of glycerol and sorbitol concentrations on mechanical, optical, and barrier properties of sweet potato starch film. NFS J. 20, 1–9.

Belhassen, R., Vilaseca, F., Mutjé, P., Boufi, S., 2014. Thermoplasticized starch modified by reactive blending with epoxidized soybean oil. Ind. Crop. Prod. 53, 261–267.

Carbonell-Verdu, A., Garcia-Garcia, D., Dominici, F., Torre, L., Sanchez-Nacher, L., Balart, R., 2017a. PLA films with improved flexibility properties by using maleinized cottonseed oil. Eur. Polym. J. 91, 248–259.

Carbonell-Verdu, A., Samper, M.D., Garcia-Garcia, D., Sanchez-Nacher, L., Balart, R., 2017b. Plasticization effect of epoxidized cottonseed oil (ECSO) on poly (lactic acid). Ind. Crop. Prod. 104, 278–286.

Collazo-Bigliardi, S., Ortega-Toro, R., Chiralt, A., 2019. Using grafted poly (ε-caprolactone) for the compatibilization of thermoplastic starch-polylactic acid blends. React. Funct. Polym. 142, 25–35.

Da Costa, J.C.M., Miki, K.S.L., da Silva Ramos, A., Teixeira-Costa, B.E., 2020. Development of biodegradable films based on purple yam starch/chitosan for food application. Heliyon 6 (4), e03718.

Ferri, J.M., Samper, M.D., García-Sanoguera, D., Reig, M.J., Fenollar, O., Balart, R., 2016a. Plasticizing effect of biobased epoxidized fatty acid esters on mechanical and thermal properties of poly (lactic acid). J. Mater. Sci. 51 (11), 5356–5366.

Ferri, J.M., Garcia-Garcia, D., Sánchez-Nacher, L., Fenollar, O., Balart, R., 2016b. The effect of maleinized linseed oil (MLO) on mechanical performance of poly (lactic acid)-thermoplastic starch (PLA-TPS) blends. Carbohydr. Polym. 147, 60–68.

Frone, A.N., Panaitescu, D.M., Chiulan, I., Nicolae, C.A., Vuluga, Z., Vitelaru, C., Damian, C.M., 2016. The effect of cellulose nanofibers on the crystallinity and nanostructure of poly (lactic acid) composites. J. Mater. Sci. 51 (21), 9771–9791.

Garcia-Garcia, D., Carbonell-Verdu, A., Arrieta, M.P., López-Martínez, J., Samper, M.D., 2020. Improvement of PLA film ductility by plasticization with epoxidized karanja oil. Polym. Degrad. Stabil. 179, 109259.

Gómez-Contreras, P., Contreras-Camacho, M., Avalos-Belmontes, F., Collazo-Bigliardi, S., Ortega-Toro, R., 2020. Improving the interfacial adhesion of biodegradable blends using epoxidized yam starch with low content of polylactic acid. Kor. J. Chem. Eng. Under Review.

Gurler, N., Paşa, S., Alma, M.H., Temel, H., 2020. The fabrication of bilayer polylactic acid films from cross-linked starch as eco-friendly biodegradable materials: synthesis, characterization, mechanical and physical properties. Eur. Polym. J. 127, 109588.

Gutiérrez, T.J., Alvarez, V.A., 2017. Data on physicochemical properties of active films derived from plantain flour/PCL blends developed under reactive extrusion conditions. Data in Brief 15, 445–448.

Herniou, C., Mendieta, J.R., Gutiérrez, T.J., 2019. Characterization of biodegradable/ non-compostable films made from cellulose acetate/corn starch blends processed under reactive extrusion conditions. Food Hydrocolloids 89, 67–79.

Khosravi, A., Fereidoon, A., Khorasani, M.M., Naderi, G., Ganjali, M.R., Zarrintaj, P., et al., 2020. Soft and hard sections from cellulose-reinforced poly (lactic acid)-based food packaging films: a critical review. Food Packaging and Shelf Life 23, 100429.

Liu, W., Qiu, J., Zhu, L., Fei, M.E., Qiu, R., Sakai, E., et al., 2018. Tannic acid-induced crosslinking of epoxidized soybean oil for toughening poly (lactic acid) via dynamic vulcanization. Polymer 148, 109–118.

Mikus, P.Y., Alix, S., Soulestin, J., Lacrampe, M.F., Krawczak, P., Coqueret, X., Dole, P., 2014. Deformation mechanisms of plasticized starch materials. Carbohydr. Polym. 114, 450–457.

Mirkhalaf, S.M., Fagerström, M., 2019. The mechanical behavior of polylactic acid (PLA) films: fabrication, experiments and modelling. Mech. Time-Dependent Mater. 1–13.

Moo-Tun, N.M., Iniguez-Covarrubias, G., 2020. Assessing the effect of PLA, cellulose microfibers and CaCO$_3$ on the properties of starch-based foams using a factorial design. Polym. Test. 86, 106482.

Muller, P., Bere, J., Fekete, E., Móczó, J., Nagy, B., Kállay, M., Pukánszky, B., 2016. Interactions, structure and properties in PLA/plasticized starch blends. Polymer 103, 9–18.

Ortega-Toro, R., Jiménez, A., Talens, P., Chiralt, A., 2014. Properties of starch hydroxypropyl methylcellulose-based films obtained by compression molding. Carbohidrate Polym. 109, 155–165.

Ortega-Toro, R., Contreras, J., Talens, P., Chiralt, A., 2015a. Physical and structural properties and thermal behaviour of starch-poly (ε-caprolactone) blend films for food packaging. Food Packaging and Shelf Life 5, 10–20.

Ortega-Toro, R., Morey, I., Talens, P., Chiralt, A., 2015b. Active bilayer films of thermoplastic starch and polycaprolactone obtained by compression molding. Carbohydr. Polym. 127, 282–290.

Ortega-Toro, R., Santagata, G., d'Ayala, G.G., Cerruti, P., Oliag, P.T., Boix, M., Malinconico, M., 2016b. Enhancement of interfacial adhesion between starch and grafted poly (ε-caprolactone). Carbohydr. Polym. 147, 16–27.

Ortega-Toro, R., Collazo-Bigliardi, S., Talens, P., Chiralt, A., 2016a. Influence of citric acid on the properties and stability of starch-polycaprolactone based films. J. Appl. Polym. Sci. 133 (2), 1–18.

Pankaj, S.K., Bueno-Ferrer, C., Misra, N.N., O'Neill, L., Jiménez, A., Bourke, P., Cullen, P.J., 2014. Characterization of polylactic acid films for food packaging as affected by dielectric barrier discharge atmospheric plasma. Innovat. Food Sci. Emerg. Technol. 21, 107–113.

Park, S.K., Bae, D.H., Rhee, K.C., 2000. Soy protein biopolymers cross-linked with glutaraldehyde. J. Am. Oil Chem. Soc. 77 (8), 879–884.

Pimentel, T., Pizzuti, L., Fakhouri, F.M., Mei, L.H.I., Fonseca, G.G., 2018. Development of multilayer films obtained from epoxidized methyl esters, polyhydroxyalkanoates and their combinations. J. Polym. Environ. 26 (4), 1661–1672.

Rodrigues, J.A., Parra, D.F., Lugão, A.B., 2005. Crystallization on films of PHB/PEG blends. J. Therm. Anal. Calorim. 79 (2), 379–381.

Sharif, A., Mondal, S., Hoque, M.E., 2019. In: Sanyang, M., Jawaid, M. (Eds.), Bio-based Polymers and Nanocomposites. Springer, London, pp. 233–254.

Sothornvit, R., Olsen, C.W., McHugh, T.H., Krochta, J.M., 2007. Tensile properties of compression-molded whey protein sheets: determination of molding condition and glycerol-content effects and comparison with solution-cast films. J. Food Eng. 78 (3), 855–860.

Sudha, G.S., Kalita, H., Mohanty, S., Nayak, S.K., 2017. Biobased epoxy blends from epoxidized castor oil: effect on mechanical, thermal, and morphological properties. Macromol. Res. 25 (5), 420–430.

Tampau, A., González-Martínez, C., Vicente, A.A., Chiralt, A., 2020. Enhancement of PLA-PVA surface adhesion in bilayer assemblies by PLA aminolisation. Food Bioprocess Technol. 13, 1215–1228.

Turco, R., Ortega-Toro, R., Tesser, R., Mallardo, S., Collazo-Bigliardi, S., Chiralt Boix, A., et al., 2019. Poly (Lactic acid)/Thermoplastic starch films: effect of cardoon seed epoxidized oil on their chemicophysical, mechanical, and barrier properties. Coatings 9 (9), 574.

Vachon, A., Pépin, K., Balampanis, E., Veilleux, J., Vuillaume, P.Y., 2017. Compatibilization of PLA/PEBA blends via reactive extrusion: a comparison of different coupling agents. J. Polym. Environ. 25 (3), 812–827.

Valencia-Sullca, C., Atarés, L., Vargas, M., Chiralt, A., 2018. Physical and antimicrobial properties of compression-molded cassava starch-chitosan films for meat preservation. Food Bioprocess Technol. 11, 1339–1349.

Yang, D., Peng, X., Zhong, L., Cao, X., Chen, W., Zhang, X., Sun, R., 2014. Green films from renewable resources: properties of epoxidized soybean oil plasticized ethyl cellulose films. Carbohydr. Polym. 103, 198–206.

Zhang, C., Garrison, T.F., Madbouly, S.A., Kessler, M.R., 2017. Recent advances in vegetable oil-based polymers and their composites. Prog. Polym. Sci. 71, 91–143.